MOLECULAR AND CELLULAR BIOLOGY, July 1984, p. 1260–1269
0270-7306/84/071260-10$02.00/0

Vol. 4, No. 7

Integration and Expression of Several Molecular Forms of Rous Sarcoma Virus DNA Used for Transfection of Mouse Cells

PAUL A. LUCIW,† HERMAN OPPERMANN,‡ J. MICHAEL BISHOP, AND HAROLD E. VARMUS*

Department of Microbiology and Immunology, University of California Medical Center, San Francisco, California 94143

Received 9 December 1983/Accepted 29 March 1984

To assess the factors required for integration and expression of retroviral DNA, we have examined viral DNA, RNA, and protein in NIH/3T3 mouse cells transformed by transfection with various forms of cloned Rous sarcoma virus (RSV) DNA. Linear RSV DNA molecules, derived from circular DNA containing two long terminal repeats (LTRs) and permuted by cleavage at the *Sac*I restriction endonuclease site in the leader sequence, were integrated near the ends of the linear molecule, with the LTRs on the 3′ side of the *src* gene. Integration of a subgenomic RSV DNA fragment containing the viral *src* gene without intact LTRs also occurred near the ends of the linear molecule. Head-to-tail tandem arrays of RSV DNA species were observed in some transformed cell lines that received fully digested DNA and in all cell lines that received DNA ligated to produce oligomers before transfection. Closed circular RSV DNA, with one or two LTRs, integrated without apparent specificity within several regions of the viral genome. After transfection with *Sac*I-permuted RSV DNA still linked to arms of the lambda bacteriophage vector DNA, bacteriophage sequences were joined to host DNA. Transformed cell lines produced by transfection with the various forms of RSV DNA produced similar levels of viral *src* protein, although the efficiency of successful transformation varied by at least two orders of magnitude. Analyses of viral polyadenylated RNA, together with the patterns of viral DNA in transformed cells, indicated that viral DNA can be integrated and expressed without regard to LTR sequences, with adjacent host DNA presumably supplying signals required for the promotion and processing of functional *src* mRNA.

Essential aspects of retrovirus replication include synthesis of DNA from an RNA genome by reverse transcription, integration of viral DNA into host cell DNA, and transcription of viral genes from the integrated provirus (2, 27). After infection of cells with retroviruses, a linear double-stranded DNA, with terminally redundant sequences (long terminal repeats [LTRs]) 300 to 1,200 base pairs (bp) in length, is synthesized from the genomic RNA by RNA-dependent DNA polymerase found in virions. A portion of the linear DNA molecules in infected cells is converted to closed circular forms, some with one copy and some with two copies of the LTR. Proviral DNA is found integrated at many sites in the host cell genome, maintains an orientation that is colinear with the unintegrated linear viral DNA, and contains a copy of the LTR at each end in covalent linkage to cell DNA; however, the mechanism of retrovirus integration has not yet been elucidated. Initiation of viral RNA synthesis occurs in the leftward (upstream) LTR, and the addition of polyadenylic acid [poly(A)] tails to viral RNA is signaled by sequences in the rightward (downstream) LTR.

We have examined the efficiency of transformation and the patterns of integration and viral gene expression after transfection of nonpermissive NIH/3T3 mouse cells with various forms of Rous sarcoma virus (RSV) DNA derived from a circular molecule cloned in *Escherichia coli* (7). The influence of the position of the LTR upon integration in the absence of viral proteins that normally accompany the viral genome into the cell and upon viral transcription was studied by transfection with several forms of cloned RSV DNA (Fig. 1): (i) viral DNA linearized and permuted by cleavage at a site located within the leader region of the RSV genome (Fig. 1A); (ii) ligated tandem arrays of permuted linear RSV DNA (Fig. 1B); (iii) recircularized viral DNA (Fig. 1C); (iv) a subgenomic DNA fragment encompassing the viral *src* gene (1,593 bp) and enhancer sequence (15) but lacking a complete LTR (Fig. 1D); and (v) chimeric DNA consisting of the permuted configuration of RSV DNA constrained within bacteriophage λ DNA (Fig. 1E).

Each of these forms of cloned RSV DNA was shown to transform NIH/3T3 mouse cells, albeit at different frequencies, and all transformed cells produced RSV *src* protein indistinguishable from that found in cells infected with virus. The LTRs of these forms of cloned retrovirus DNA were not directly involved in integration into host cell DNA after transfection. Whenever linear forms of retrovirus DNA were used to transform cells, integration into cell DNA occurred near the ends of the linear molecules. Closed circular forms of retrovirus DNA were shown to integrate at several sites within viral DNA. Examination of integration patterns and viral RNA transcripts in cells transformed by each of these forms of cloned RSV DNA revealed that the LTRs are not obligatory for transcription of RSV genes; cellular sequences appear to play a role in initiation or processing or both of viral transcripts in situations not allowing the use of viral signals.

(Preliminary accounts of this work were presented at the Cold Spring Harbor RNA Tumor Virus Meetings of 1980 and 1981).

MATERIALS AND METHODS

Cell culture and transfection. NIH/3T3 mouse cells, provided by G. M. Cooper, Sidney Farber Cancer Institute, Harvard Medical School, Boston, Mass., were propagated in monolayer culture in Dulbecco minimal essential medium (DMEM) supplemented with 10% calf serum. Anderson et al. (1) first described the use of these cells for studying cellular transformation by DNA transfection. Coprecipitates

* Corresponding author.
† Present address: Chiron Corp., Emeryville, CA 94608.
‡ Present address: Genentech, Inc., South San Francisco, CA 94080.

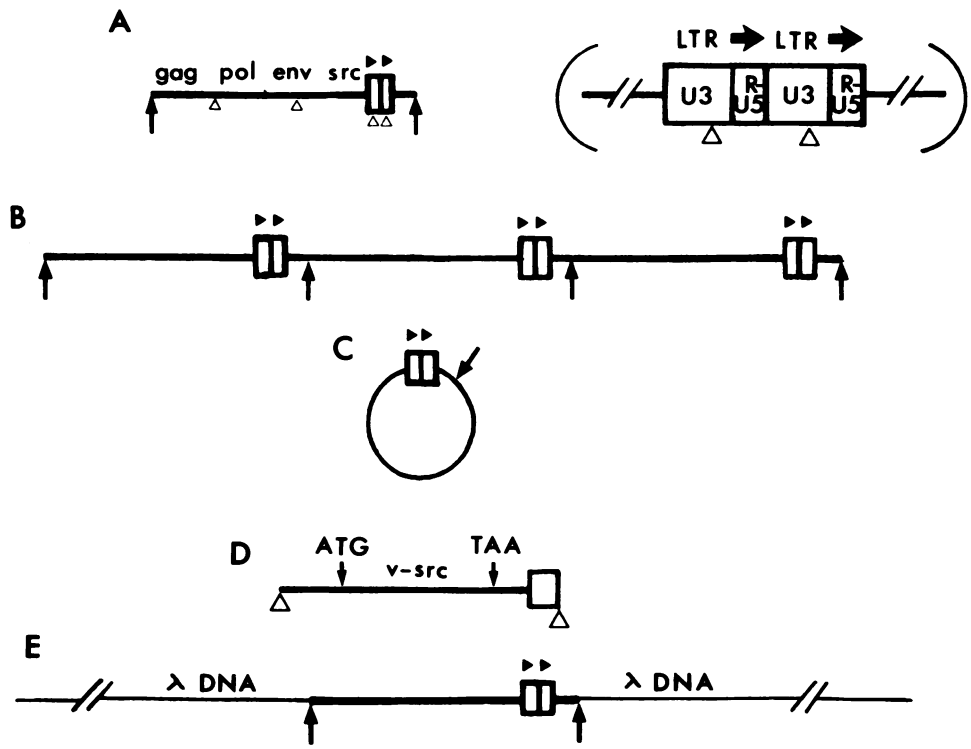

FIG. 1. Forms of cloned RSV DNA used for transfection. The bold lines represent RSV DNA sequences. Open boxes represent LTR regions; solid triangles above the LTRs indicate the direction of transcription. The open triangles show the locations of *Eco*RI cleavage sites, and the unmarked arrows indicate the locations of *Sac*I cleavage sites. (A) 9.4-kb *Sac*-I permuted linear RSV DNA. The inset to the right is an enlargement of the LTR region divided into U3 and R-U5 portions; the large arrows denote the direction of transcription. (B) Tandem arrays of *Sac*I-permuted linear RSV DNA. (C) Closed circular RSV DNA (9.4 kb). (D) Subgenomic (3-kb) *Eco*RI v-*src* DNA fragment, showing *src* initiation and termination codons. (E) Chimeric λ/RSV DNA containing a complete (9.4-kb) *Sac*I-permuted RSV DNA.

of DNA and calcium were prepared by the method of Graham and Van der Eb (10), using HEPES (*N*-2-hydroxyethylpiperazine-*N'*-2-ethanesulfonic acid)-buffered saline. A 0.5-ml volume of precipitate, containing a total of 10 μg of DNA, was applied directly to a 60-mm plastic tissue culture dish containing ca. 500,000 NIH/3T3 cells in 5 ml of DMEM with 10% fetal calf serum. We found that when the DNA-calcium coprecipitate was added to DMEM containing calf serum (several lots were tested), a massive precipitate formed immediately that was toxic to the monolayer of NIH/3T3 cells. When fetal calf serum was used instead of calf serum in DMEM during transfection, a very fine precipitate was observed, and the cells appeared to be healthy. The tissue culture dishes containing the DNA-calcium coprecipitate were incubated 6 to 8 h at 37°C in a CO_2 incubator (95% air, 5% CO_2), the medium was removed by aspiration, and the cell monolayers were treated at room temperature with 1 ml of an adjuvant consisting of a 15% glycerol solution made up in HEPES-buffered saline (3, 23). After 4 min, the glycerol solution was removed by aspiration, and 5 ml of DMEM containing 10% calf serum was added. The monolayers were placed in a 37°C CO_2 incubator and fed with fresh growth medium every 2 days. Low-power microscopy (×40) was used to detect foci of transformed cells. A focus consisted of a compact area of large, rounded and refractile cells growing on a background of flat, untransformed NIH/3T3 cells (5). Transformed foci were first noticed at 12 to 14 days and were counted at 20 to 24 days after transfection. Colonies of transformed cells containing more than 100 cells were picked with a drawn-out Pasteur pipette, transferred to microtiter wells, and propagated. For single-cell cloning, transformed cells originating from one colony were trypsinized and seeded at one cell per well and propagated; microscopic observation was used to identify microtiter wells containing cells originating from a single cell.

Preparation of cellular and cloned viral DNAs. High-molecular-weight cellular DNA was prepared by resuspending cultured cells at 10^6/ml in a buffer containing 20 mM Tris-hydrochloride (pH 7.6), 10 mM EDTA, 100 mM NaCl, 0.5% sodium dodecyl sulfate, and 200 μg of pronase (Calbiochem-Behring; stock solution at 10 mg/ml in 10 mM Tris-hydrochloride [pH 7.6]–10 mM EDTA and predigested for 2 h at 37°C) per ml. After incubation at 37°C for 2 h (or overnight at room temperature), the DNA was deproteinized by extraction three to four times with an equal volume of a 1:1 phenol-chloroform mixture (preequilibrated with an aqueous solution containing 100 mM Tris-hydrochloride (pH 7.6), 10 mM EDTA, and 0.01% β-mercaptoethanol). After the final extraction, the NaCl concentration was adjusted to 300 mM; then 3 volumes of cold ethanol (−20°C) was layered on top, and the tube was capped and inverted rapidly 8 to 10 times to collapse the DNA fibers. The DNA was recovered as a pellet after a low-speed centrifugation (2,000 to 5,000 × *g* for 10 min). Occasionally, instead of the centrifugation step, the DNA was spooled on a glass rod. The DNA precipitate was resuspended in water, and an equal volume of a solution containing 50 mM Tris-hydrochloride (pH 7.6) and 20 mM EDTA was added; to this, pancreatic RNase (stock solution at 10 mg/ml in water pretreated at 80°C for 30 min or boiled for 10 min) was added to a final concentration of 100 μg/ml.

After incubation at 37°C for 1 h, predigested pronase was added to a final concentration of 100 μg/ml, and incubation was continued at 37°C for 1 h. Two extractions were performed with equal volumes of a 1:1 phenol-chloroform mixture as described above; these extractions were followed by two extractions with chloroform. The final aqueous phase was adjusted to 300 mM NaCl, and the DNA was precipitated with cold ethanol (see above). After two washes with cold 70% ethanol, the DNA precipitate was allowed to drain and then resuspended in sterile glass-distilled water at a final DNA concentration of 500 μg/ml. High-molecular-weight NIH/3T3 cell DNA prepared in this fashion was passed twice through a 22-gauge syringe before use as carrier DNA for transfection.

The preparation of chimeric phage (λgt · WES)-RSV DNA is described by DeLorbe et al. (7). This DNA was digested with *Sac*I, and the 9.4-kilobase (kb) linear RSV DNA was separated from the large phage vector arms by rate-zonal centrifugation in sucrose gradients. This purified RSV DNA was digested with *Eco*RI, and the 3-kb DNA fragment encoding the v-*src* gene was cloned into the *Eco*RI site of λgt · WES (W. DeLorbe, unpublished data). This cloned phage-RSV *src* chimeric DNA was used as a source of the 3-kb v-*src* DNA fragment. After digestion of this chimera with *Eco*RI, the 3-kb *src* DNA fragment was separated from the phage vector DNA by rate-zonal sedimentation in sucrose gradients (described above). Closed circular RSV DNA was prepared by ligating purified *Sac*I-permuted linear RSV DNA at a low DNA concentration (5 μg/ml) in 10 mM Tris-hydrochloride (pH 7.6)–10 mM NaCl–10 mM $MgCl_2$–5 μg of ethidium bromide per ml with 100 U of T4 DNA ligase at 4°C for 18 h (19). After the reaction, the DNA solution was adjusted to 300 mM NaCl (with a 4 M NaCl stock solution) and 10 mM EDTA (with a 0.25 M stock solution) and extracted four times with equal volumes of *n*-butanol (previously saturated with water). Closed circular DNA was separated from other DNA forms by two extractions with acid-phenol (29). Analysis by agarose gel electrophoresis revealed that more than 90% of this DNA was in the closed circular configuration (P. A. Luciw, unpublished data).

TABLE 1. Efficiency of transformation by forms of RSV DNA

Form of RSV DNA[a]	No. of foci per 60-mm dish, each containing the following amt of RSV DNA (μg)[b]:				Rescuable virus[e]
	0.001[c]	0.01[c]	0.1[c]	10[d]	
9.4-kb *Sac*I-permuted linear DNA (A)	2	12	17	8	+ and −
Tandem arrays of *Sac*I-permuted linear DNA (B)	10	16	15	9	+ and −
Closed circular DNA (two LTRs) (C)	1	9	12	ND	ND
Subgenomic 3-kb v-*src* DNA fragment (D)	0.3	3	11	2	ND
Chimeric λ/RSV DNA (E)	0	0	3	2	−
Proviral DNA[f]	ND	ND	ND	2	+

[a] The letters in parentheses after the first five forms of RSV DNA correspond to sections A through E, respectively, of Fig. 1; see the legend to Fig. 1 for more detailed descriptions of forms.

[b] The number of foci per 60-mm dish given here is the average from two or three experiments; six to eight dishes per form of DNA were used in each experiment. Each dish was seeded with 500,000 NIH/3T3 mouse cells 1 day before transfection as detailed in the text.

[c] NIH/3T3 cell DNA was used as the carrier.

[d] No carrier cell DNA was applied.

[e] +, Infectious RSV recovered after cocultivation of transfected mammalian cells with chicken embryo cells; −, no infectious RSV recovered.

[f] DNA (10 μg) from NIH/3T3 cells containing one RSV provirus.

Preparation of ^{32}P-labeled probes and analysis of cellular DNA, RNA, and protein. To prepare ^{32}P-labeled probe representative of the whole genome (RSV_{rep} probe), cloned linear RSV DNA was denatured by boiling for 3 min in a solution containing 5 mM Tris-hydrochloride (pH 7.6)–1 mM EDTA in a polypropylene tube. The denatured DNA was then incubated with calf thymus primers, [α-^{32}P]dCTP, and reverse transcriptase (supplied by J. Beard) as described by Shank et al. (21). A probe specific to the *gag* region was made by using as template the 1.3-kb *Bam*HI DNA fragment obtained by agarose gel purification of a *Bam*HI digest of the cloned linear *Sac*I-permuted RSV DNA. The 3-kb *src* DNA fragment purified as described above was used as template for probe for the v-*src* gene. ^{32}P-labeled RSV-U5 probe was made in the endogenous reaction with purified PR-C virus, and ^{32}P-RSV-U3 probe was made by purified reverse transcriptase from a purified RSV (Schmidt-Ruppin [SR]-A strain) RNA template and oligodeoxythymidylic acid primer (21). Integration patterns in cellular DNA were analyzed by gel electrophoresis and Southern blotting as detailed by Hughes et al. (12). Poly(A)-containing RNA was prepared from transformed cells and analyzed by agarose gel electrophoresis and blotting to nitrocellulose membranes (16). Immunoprecipitation of metabolically labeled viral gene products was performed as described by Oppermann et al. (17).

RESULTS

Efficiency of transformation of NIH/3T3 mouse cells with cloned RSV DNA. Table 1 presents the efficiencies of formation of transformed cell foci after transfection of NIH/3T3 mouse cells with the several forms of cloned RSV DNA illustrated in Fig. 1. Cellular DNA from an NIH/3T3 transformed mouse cell harboring one copy of RSV provirus (ca. 0.1 pg of RSV DNA per μg of cellular DNA) was used as a standard for comparisons; ca. 10 to 20 foci per plate were generally observed by using 20 μg of cellular DNA with five proviruses per cell (data not shown). *Sac*I-permuted cloned linear RSV DNA in the presence of carrier DNA was ca. 1,000-fold less efficient in inducing focus formation than was proviral DNA, on the basis of number of viral DNA molecules. Saturation for focus formation per 5×10^5 cells occurred at 10 to 15 foci, suggesting that only a small number of cells were competent to assimilate DNA and undergo transformation.

The relatively low transformation efficiency of *Sac*I-permuted linear RSV DNA might be due to the fact that the viral LTRs are not properly positioned in relation to the viral genes for efficient integration or transcription or both. To bracket the viral genes with LTR sequences, tandem arrays of the *Sac*I-permuted linear RSV DNA were made in vitro with T4 DNA ligase. Electrophoretic analysis on agarose gels showed that the tandem arrays were composed of four to six unit molecules; as expected, 50% of the units in the tandem array were joined in a head-to-tail arrangement (viral genes now flanked by LTRs as in a normal provirus), with the remainder equally represented as head-to-head and tail-to-tail arrangements (data not shown). The transfection efficiency was approximately fivefold greater on a mass basis for tandem arrays than for *Sac*I-permuted linear RSV DNA. On a molar basis, tandem arrays are ca. 25 times more efficient in transformation than are monomers of *Sac*I-permuted linear RSV DNA but still ca. 50-fold less efficient than proviral DNA.

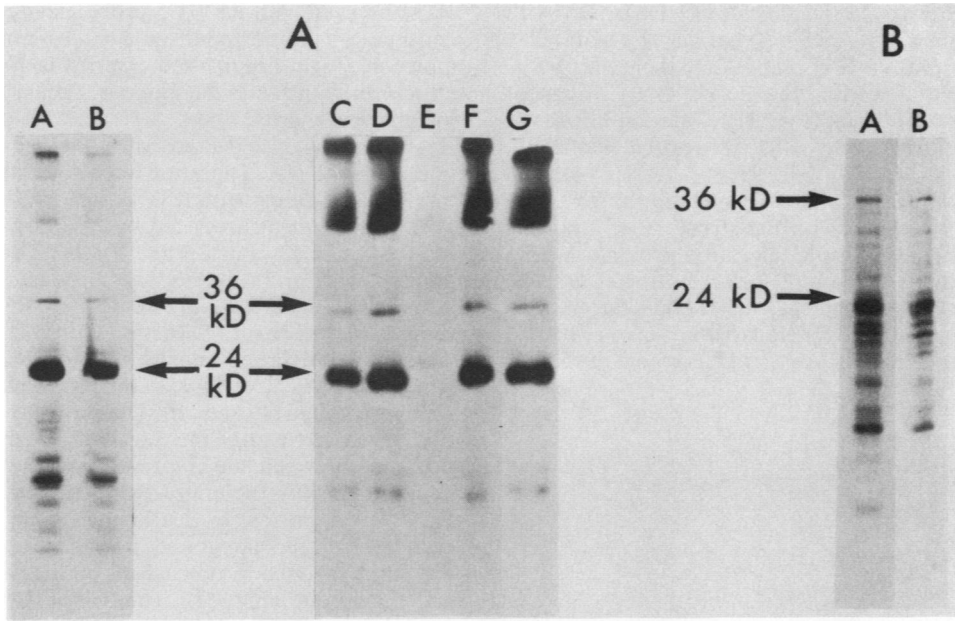

FIG. 2. Analysis of RSV polypeptides in transformed NIH/3T3 mouse cells. (A) Transformed NIH/3T3 cells, normal NIH/3T3 cells, and chicken embryo fibroblasts infected by SR-A virus were labeled in vivo with $^{32}P_i$. Cell extracts were prepared and immunoprecipitated with tumor-bearing rabbit sera. These immunoprecipitates were electrophoresed on polyacrylamide gels. Polypeptides in the region of the gel corresponding to 60 kilodaltons (kd) were recovered and treated with V8 protease, and the digestion products were electrophoresed on polyacrylamide gels. Molecular weight positions were determined by coelectrophoresing proteins of known molecular weight. The cell line and form of transfecting DNA, if any, of each lane are, respectively: A, S-d, *Sac*I-permuted linear; B, RSV-infected chicken embryo fibroblasts; C, L-8, tandem arrays of *Sac*I-permuted linear; D, E-e, 3-kb v-*src* fragment; E, uninfected NIH/3T3; F, Sc-2, closed circular DNA; G, λ-C, chimeric λ/RSV. (B) Cell line S-d (lane A) and RSV-infected chicken embryo fibroblasts (lane B) were labeled in vivo with [^{35}S]methionine. Cell extracts were prepared and then immunoprecipitated with tumor-bearing rabbit sera and the immunoprecipitates were electrophoresed on polyacrylamide gels. A polypeptide at 76 kilodaltons in each sample was recovered and then treated with papain, and the digestion products were electrophoresed on polyacrylamide gels along with marker proteins of known molecular weight.

The 3-kb *Eco*RI fragment containing v-*src* was about two- to eightfold less efficient than the *Sac*I-permuted linear RSV DNA. Transformation efficiency was markedly reduced when the *Sac*I-permuted RSV DNA was presented to cells as a chimeric DNA still linked to bacteriophage DNA.

Transformed cell lines contain pp60$^{v\text{-}src}$. To validate the claim that the foci were caused by expression of RSV DNA, transformed NIH/3T3 mouse cell lines made by transfection with each form of cloned RSV DNA were examined for production of viral proteins. pp60^{src} was tentatively identified by immunoprecipitation with antisera from tumor-bearing rabbits (data not shown) and more rigorously identified by partial digestion with V8 protease (Fig. 2A; 17). The products of pp60$^{v\text{-}src}$ from each transformed mammalian cell line are indistinguishable from the products of pp60$^{v\text{-}src}$ from chicken cells infected with SR-A virus (Fig. 2A, lane B). In some transformed mouse cell lines, immunoprecipitation with antisera from tumor-bearing rabbits revealed a protein that coelectrophoresed with Pr76^{gag} (data not shown). Analyses of papain digestion products demonstrated that the 76-kilodalton protein from mouse cells transformed by *Sac*I-permuted linear RSV DNA was indistinguishable from Pr76^{gag} made in chicken cells infected with SR-A-2 virus (Fig. 2B). Thus the *gag* gene, beginning 113 bp from the *Sac*I site (11), appears to be intact and expressed in this cell line (see below). Other viral proteins (processed *gag* proteins, *env* glycoproteins, Pr180$^{gag\text{-}pol}$, and processed products of *pol*) were not detected.

Organization of RSV DNA in cells transfected with *Sac*I-permuted linear RSV DNA. High-molecular-weight DNA from each of 17 independent NIH/3T3 mouse cell lines transformed by transfection with *Sac*I-permuted linear RSV DNA in the presence of carrier cell DNA was analyzed by restriction enzyme digestions and annealing with viral probes. Eleven cell lines contained multiple integrated copies of the *Sac*I-permuted RSV genome. Six cell lines were found to harbor a single copy of integrated RSV DNA (data not shown). A detailed analysis of one such cell line (S-d) is presented below. In each of these six cell lines, integration occurred near the ends of the linear *Sac*I-permuted RSV DNA. The *Sac*I site in the RSV genome was not restored at either end of the integrated RSV DNA molecule. The junction fragments (joining of the RSV genome to cell DNA) were unique to each cell line, indicating that integration involved different locations in cell DNA in each cell line. In one transformed cell line, ca. 900 bp from the 3′ end of the *Sac*I-permuted RSV DNA (including both LTRs) was deleted in the integrated RSV DNA.

Undigested DNA from cell line S-d did not demonstrate the presence of any free RSV-specific DNA (data not shown). Digestion with *Kpn*I, a restriction endonuclease that cleaves RSV DNA once, approximately in the middle of the genome, produced two RSV-specific DNA fragments of 6.5 and 7.0 kb (Fig. 3A), demonstrating that one copy of the RSV genome is integrated in cell line S-d. The 6.5-kb DNA fragment contains sequences from the right end of the RSV genome since it anneals with RSV-*src* probe (Fig. 3B). Digestion with *Sac*I produced a single RSV-specific DNA fragment of 11 kb (Fig. 3C), implying that at least one of the *Sac*I sites is absent. (The faint, slowly migrating band in this

lane is probably due to partial digestion.) Digestion with *Eco*RI and annealing with RSV_{rep} probe showed three bands: 15, 3.6, and 3.0 kb (Fig. 3D). Annealing with RSV-*gag* probe demonstrated that the 15-kb DNA fragment contains RSV *gag* sequences (Fig. 3E). The 3.0-kb *Eco*RI DNA fragment anneals with RSV-*src* probe (data not shown).

To compare more precisely the organization of the integrated DNA in cell line S-d with the structure of a normal provirus, we analyzed the *Eco*RI digestion products with a probe specific for the U5 region of the LTR. RSV-U5 probe detected a 330-bp DNA fragment, indicating that the two LTRs in the *Sac*I-permuted RSV linear DNA have remained joined to each other (Fig. 3H). An *Eco*RI fragment at 15 kb is also observed with RSV-U5 probe. Thus, the RSV DNA in cell line S-d is integrated as a *Sac*I-permuted linear DNA molecule (Fig. 3) in marked contrast to the typical provirus structure, with LTRs flanking viral genes, observed in cells infected with virus.

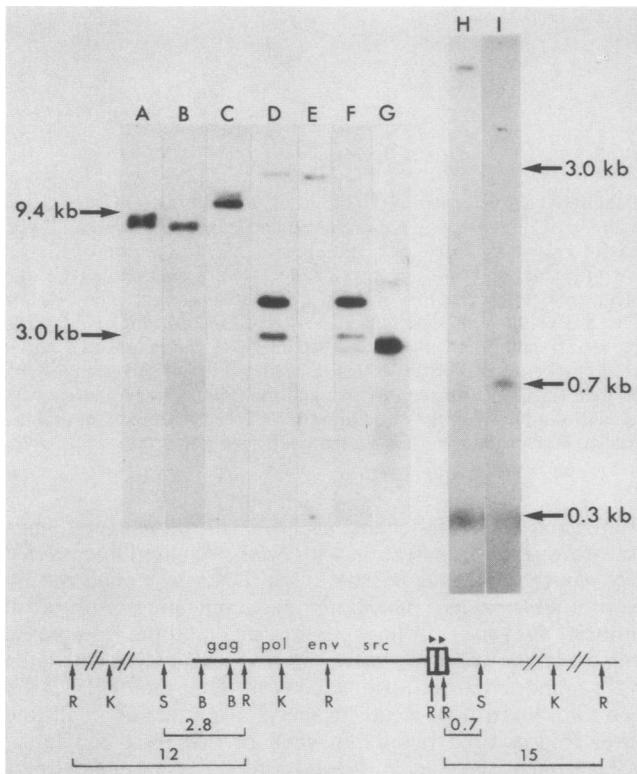

FIG. 3. Pattern of integrated RSV DNA in an NIH/3T3 cell line transformed with *Sac*I-permuted linear RSV DNA. High-molecular-weight DNA from cell line S-d was digested with a variety of restriction endonucleases, and the digestion products were electrophoresed on agarose gels and blotted by the method described by Southern (22). Several ^{32}P-labeled probes were prepared to represent specific regions of the RSV genome. The positions of markers were derived from the migration pattern of RSV DNA fragments produced by *Eco*RI digestion of DNA from mammalian cells infected with RSV. Shown here is a schematic drawing of RSV DNA (heavy line) integrated into mouse cell DNA (light lines). The open boxes represent LTRs; solid triangles above the LTRs indicate the direction of transcription. Symbols for restriction endonuclease sites: R, *Eco*RI; B, *Bam*HI; K, *Kpn*I; S, *Sac*I. The molecular distances between selected restriction endonuclease sites are in kb pairs. The restriction endonuclease(s) and RSV probe for each lane are, respectively: A, *Kpn*I, rep; B, *Kpn*I, *src*; C, *Sac*I, rep; D, *Eco*RI, rep; E, *Eco*RI, *gag*; F, *Eco*RI plus *Sac*I, rep; G, *Eco*RI plus *Sac*I, *gag*; H, *Eco*RI, R-U5; I, *Eco*RI plus *Sac*I, R-U5.

Attention was next focused on the ends of the integrated linear RSV DNA. Digestion with a mixture of *Eco*RI and *Sac*I and annealing with RSV rep probe showed that the 12-kb DNA fragment produced by *Eco*RI digestion alone was reduced to 2.8 kb (Fig. 3D and F); this 2.8-kb DNA fragment anneals with probe to RSV *gag*-specific probe (Fig. 3G). Thus, the left end of the integrated RSV DNA has not retained the *Sac*I site. Digestion with *Bam*HI and annealing with RSV rep probe and RSV *gag*-specific probe demonstrated the presence of a 1.3-kb DNA fragment encoding *gag* sequences (data not shown). These results show that integration of the left end of the *Sac*I-permuted linear RSV DNA occurred between the *Sac*I site and the proximal *Bam*HI site; presumably the entire *gag* gene remained intact since $Pr76^{gag}$ was present in this line (Fig. 2B). To focus on the right end of the integrated RSV DNA, we analyzed the digestion products produced by both *Eco*RI and *Sac*I with RSV-U5 probe (Fig. 3I). The 330-bp DNA fragment, observed previously, confirms that the two LTRs remain joined to each other. The 700-bp DNA fragment represents the joining of the right end of the *Sac*I-permuted RSV DNA to cell DNA; this fragment represents, at most, 320 bp of viral DNA; the remainder is cell DNA up to a cellular *Sac*I site. The viral junction lies between the *Sac*I site at the right end of unintegrated RSV DNA and the proximal *Eco*RI site.

The diagram in Fig. 3 shows the organization of integrated RSV DNA in cell line S-d. As might be anticipated, no infectious virus was rescued by cocultivating chicken embryo fibroblasts with this line or with any of the six transformed cell lines containing one integrated copy of the *Sac*I-permuted RSV genome (Table 1). The manner in which these permuted genomes are expressed to produce $pp60^{src}$ will be considered in a subsequent section.

Eleven additional transformed cell lines were found to contain multiple copies of integrated RSV DNA. Restriction endonucleases that cleave RSV DNA only once (*Kpn*I, *Hpa*I, and *Sal*I) were used to digest high-molecular-weight DNA from these cell lines. Each of these digestions yielded a genome-length 9.4-kb RSV DNA fragment as well as several other RSV species (unpublished data). These patterns are consistent with integration of a tandem array(s) containing units of the *Sac*I-permuted RSV DNA joined together in a head-to-tail fashion. No DNA fragments were seen that would have been characteristic of a head-to-head or tail-to-tail joining (see below). In 9 of these 11 cell lines, digestion with *Sac*I revealed the presence of a major RSV DNA species at 9.4 kb; thus, *Sac*I-permuted linear RSV DNA molecules were directly ligated to each other inside the cell. In two cell lines possessing tandem arrays, *Sac*I digestion produced RSV DNA fragments greater than 9.4 kb; in these cell lines, RSV sequences at the ends of the *Sac*I-permuted linear RSV DNA molecules were probably lost before or during intracellular ligation.

Transformed lines containing tandem units of RSV DNA yielded infectious RSV after fusion with permissive chicken cells (Table 1). To determine the consequences of the integration pattern on the structure of these viruses, we examined the structure of proviral DNA in the chicken cells infected with each of these viruses. The *Sac*I site was present in viruses recovered from the cell lines containing tandem arrays of RSV DNA units joined at intact *Sac*I sites

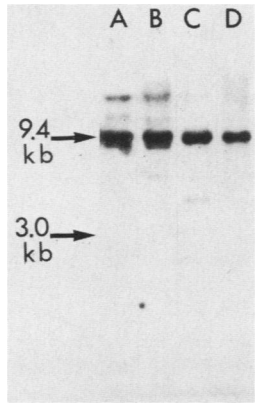

FIG. 4. Pattern of integrated RSV DNA in an NIH/3T3 mouse cell line transformed by tandem arrays of the *Sac*I-permuted RSV genome. High-molecular-weight DNA was prepared from cell line L8 and analyzed as described in the legend to Fig. 3. RSV_{rep} probe was used to detect RSV DNA in the following restriction endonuclease digest: lane A, *Sac*I; lane B, *Kpn*I; lane C, *Hpa*I; lane D, *Sal*I.

(P. Luciw, J. M. Bishop, and H. E. Varmus, unpublished data). In contrast, the *Sac*I site was absent in the virus rescued from the two cell lines that appeared to have lost the *Sac*I site at the point of joining of two *Sac*I linear RSV DNA molecules (unpublished data). The physiological effects of these presumed deletion mutations in the leader sequence have not been further studied.

Integrated DNA in cells transformed with tandem arrays of RSV DNA. The integrated tandem arrays in 12 cell lines transformed with *Sac*I-permuted RSV DNA molecules ligated in vitro with T4 DNA polymerase were compared with the tandem arrays in the transfecting DNA species. The analysis of DNA from one such cell line, L8, with restriction enzymes that cleave RSV DNA once shows an integrated tandem array composed of the *Sac*I-permuted RSV genome joined head to tail (Fig. 4). The fragments predicted to result from head-to-head or tail-to-tail joinings (e.g., a 5-kb *Sal*I fragment) were not observed, although these made up one-half of the joinings in the tamdem arrays prepared in vitro. Similar restriction endonuclease mapping studies with five other cell lines revealed integrated tandem arrays composed only of head-to-tail joinings of the *Sac*I-permuted RSV DNA molecules.

Virus was rescued by cocultivation with permissive chicken cells from 11 of 12 transformed NIH/3T3 mouse cell lines made after transfection with tandem arrays, including cell line L8 (Table 2). The one transformed cell line that did not yield rescuable virus contained only a fragment of the RSV *Sac*I-permuted DNA (unpublished data).

Integration of closed circular RSV DNA after transfection. The experiments presented thus far indicate that the LTRs do not dictate the site of integration within permuted linear RSV DNA molecules during transfection. Supercoiled retroviral DNA molecules have been identified in tissue culture cells infected with virus and may represent a precursor to proviral DNA (27). Cloned *Sac*I-permuted linear RSV DNA, containing two complete copies of the LTR sequence (25), was converted to a closed circular configuration in vitro with T4 DNA ligase. The transformation efficiency of NIH/3T3 mouse cells with closed circular RSV DNA was approximately one focus per nanogram of RSV DNA, a value similar to the transformation frequency obtained with *Sac*I-permuted linear RSV DNA (Table 1).

Restriction enzyme digestions showed that each of nine cell lines transformed with closed circular DNA contained several copies of complete or incomplete RSV DNA linked to high-molecular-weight cell DNA. Analysis of DNA in these cell lines with probes for RSV LTR sequences demonstrated that at least some of the inserted DNA molecules in each cell line contained an intact LTR circle junction (Table 1). Digestion of DNA from cell line Sc-2 with *Kpn*I yielded at least eight DNA bands (Fig. 5A), none of which migrated at genome length; thus this cell line appears to contain multiple copies of integrated RSV DNA, not arranged as a tandem array. Digestion of high-molecular-weight DNA from cell line Sc-2 with *Pvu*I, an enzyme that cleaves RSV DNA once within the LTR, also yielded several DNA fragments, again none of 9.4 kb (Fig. 5B). In contrast, *Pvu*I digestion of integrated RSV proviruses in cells infected with RSV produces a fragment at 9.4 kb (Fig. 5C). Attention was directed to the role of the LTR sequence in integration of supercoiled RSV DNA in cell line Sc-2. Digestion of high-molecular-weight DNA with *Eco*RI and annealing with RSV_{rep} probe revealed a complex pattern (Fig. 5D). To focus specifically on the RSV LTR sequence, the *Eco*RI digest was annealed with RSV-U5 probe. Notably, a DNA fragment of 330 bp was observed (Fig. 5E). Thus, the tandem LTRs remained intact in at least one copy of integrated RSV DNA. These

TABLE 2. Summary of integrated forms of transfected DNA

Form of transfected DNA[a]	No. of lines studied	Characteristics of integrated RSV DNA	Examples shown
A	6	Single copy joined near ends; *Sac*I sites lost	S-d (Fig. 3)
	2	Head-to-tail tandems without *Sac*I sites	
	9	Head-to-tail tandems with *Sac*I sites	
B	11	Head-to-tail tandems with *Sac*I sites	L8 (Fig. 4)
	1	Subgenomic fragment of RSV DNA	
C	9	Multiple copies, varied insertion sites in viral DNA	Sc-2 (Fig. 5)
D (without carrier DNA)	2	Two copies inserted in head-to-tail arrangement, with *Eco*RI site at junction	
	1	Two copies, head to tail without *Eco*RI site	
	3	Multiple head-to-tail insertions	
D (with carrier DNA)	1	Single copy inserted near ends	E-e (Fig. 6)
	5	Multiple copies, some head to tail	
	12	Multiple copies, no tandems	
E	1	Insertion within bacteriophage DNA arms	λ-C

[a] See the legend to Fig. 1 for definition of DNA forms used for transfection; the letters here correspond to sections in Fig. 1.

results show that cell line Sc-2 does not harbor any RSV DNA insertions similar in structure to proviruses in cells infected with virus. Annealing of the *Pvu*I digest of cell line Sc-2 (Fig. 5B) with RSV-U5 probe also demonstrated a 330-bp DNA fragment, representing the junction of two LTR sequences (data not shown).

Transformation of NIH/3T3 mouse cells with a subgenomic RSV DNA fragment in the presence and absence of carrier DNA. All of the forms of cloned RSV DNA used to transfect cells in the previous experiments contained a complete LTR as well as intact *gag*, *pol*, *env*, and *src* genes. To study the requirements for expression of viral *src*, we prepared a 3-kb subgenomic DNA fragment (produced by *Eco*RI digestion of cloned *Sac*I-permuted RSV DNA); this fragment contains a complete *src* gene, the splice acceptor site preceding *src*, and part of the first RSV LTR.

The transformation efficiency after transfection of NIH/3T3 cells with this fragment was about one-fourth of that obtained with the *Sac*I-permuted RSV DNA (Table 1). An analysis of the integration pattern in one transformed cell line, E-e, is presented here. No free RSV DNA was detected in undigested DNA from cell line E-e (Fig. 6A). Digestion with *Sac*I, a restriction endonuclease that does not cleave within the 3-kb fragment, yielded one band at 8 kb, suggested a single insertion (Fig. 6B). Digestion with *Eco*RI yielded one band at 12 kb (Fig. 6C), implying that at least one terminal *Eco*RI site was lost. A restriction endonuclease, *Bgl*I, that cleaves only once within the 3-kb *src* DNA

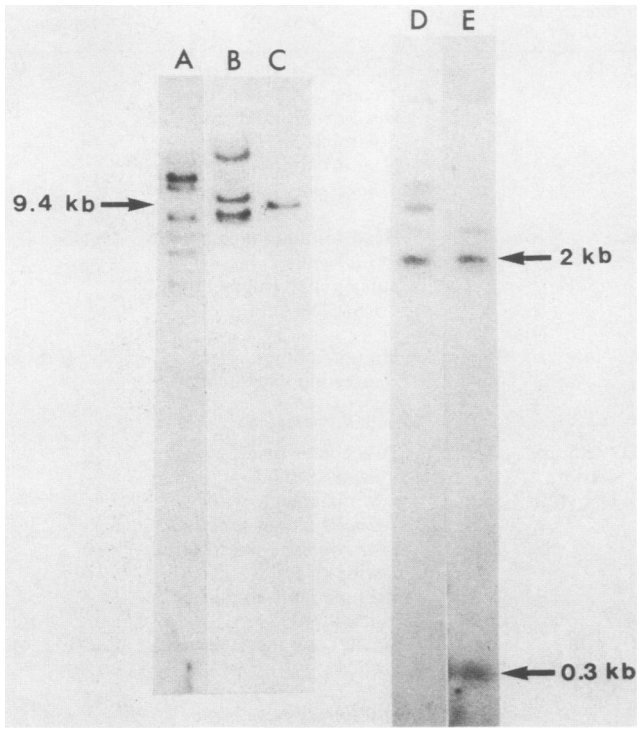

FIG. 5. RSV DNA in a cell line transformed by closed circular form of cloned RSV DNA. The pattern of integrated RSV DNA in transformed cell line Sc-2 (lanes A, B, D, and E) was analyzed as described in the legend to Fig. 3. Shown here are the following restriction endonuclease digests analyzed with probes to RSV sequences: lane A, *Kpn*I, RSV_{rep} probe; lane B, *Pvu*I, RSV_{rep} probe; lane D, *Eco*RI, RSV_{rep} probe; lane E, *Eco*RI, R-U5 probe. Lane C contains a *Pvu*I digest of DNA from an RSV-infected mouse cell containing a normal provirus, detected with RSV_{rep} probe.

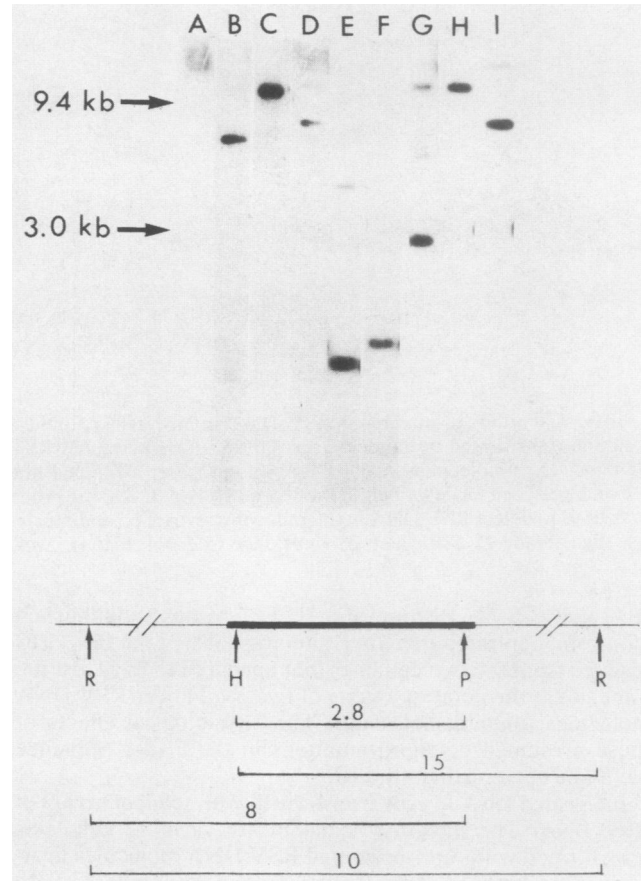

FIG. 6. Integrated RSV DNA in an NIH/3T3 cell line transformed by transfection with the subgenomic (3-kb) *Eco*RI RSV DNA fragment encoding v-*src*. High-molecular-weight DNA was prepared from cell line E-e and analyzed as described in the legend to Fig. 3. Probe specific to v-*src* was used for annealing to the following restriction endonuclease digestions: lane A, undigested; lane B, *Sac*I; lane C, *Eco*RI; lane D, *Bgl*I; lane E, *Eco*RI plus *Bgl*I; lane F, *Sma*I; lane G, *Pvu*II; lane H, *Hin*dII plus *Eco*RI; lane I, *Pvu*I plus *Eco*RI. The schematic drawing shows integrated RSV DNA (heavy line) in host cell DNA (light lines) along with several restriction endonuclease sites (R, *Eco*RI; H, *Hin*dIII; P, *Pvu*I). The numbers represent distances between restriction endonuclease sites in kb pairs.

molecule, produced two bands at 8 and 11 kb (Fig. 6D). These two bands represent the joining of each end of the 3-kb *src* DNA fragment to cellular or carrier DNA. Thus, cell line E-e contains one integrated copy of the 3-kb *src* DNA molecule. Analysis with each of two restriction endonucleases that cleave several times within the 3-kb *src* DNA fragment, *Sma*I and *Pvu*I, demonstrated the expected internal DNA fragments (Fig. 6E and F); no rearrangements were detectable within the inserted RSV DNA fragment. The *Hin*dIII site, 100 bp from the left end, and the *Pvu*I site, 200 bp from the right end, are present, since a digestion with a mixture of *Hin*dIII and *Pvu*I yielded a 2.7-kb DNA fragment (Fig. 6G). Digestion with a mixture of *Hin*dIII and *Eco*RI or with a mixture of *Pvu*I and *Eco*RI yielded a major DNA fragment in each case that was larger than 3 kb (Fig. 6H and I), indicating that an *Eco*RI site was not present at either end of the integrated fragment.

The integration pattern was examined in each of a total of

18 transformed cell lines made by transfecting with nanogram amounts of the 3-kb RSV *src* DNA species. In addition to cell line E-e shown above to contain one integrated copy, 14 transformed cell lines contained between two and approximately five integrated copies. The remaining three cell lines had many, perhaps as many as 20, integrated copies (data not shown). Of the total of 17 cell lines with multiple copies, 5 were found to possess tandem arrays; the 3-kb *src* DNA units in these tandem arrays were invariably joined in a head-to-tail orientation (data not shown).

In the experiments described earlier, the issue as to whether the transfecting DNA species inserted into the carrier DNA or directly into the recipient cell genome remained unresolved, since carrier DNA from NIH/3T3 cells was present. Six of six independent transformed cell lines made by transfection with the 3-kb *src* DNA fragment in the absence of carrier DNA were found to contain integrated tandem arrays. Two of these six cell lines had an integrated head-to-tail dimer of the 3-kb *src* DNA fragment; in both of these cell lines the *Eco*RI site was present at the junction of the two units in the integrated dimer (data not shown). Of the remaining four cell lines, one contained an integrated head-to-tail dimer; however, no *Eco*RI site was present at the junction of the two units in the integrated dimer. The remaining three cell lines presented complex patterns; each had three or more integrated units of the 3-kb *src* DNA fragment arranged in head-to-tail tandem arrays; there was no evidence of head-to-head or tail-to-tail joining of the 3-kb *src* DNA fragment in any of these six cell lines (see below).

Transfection with chimeric λ/RSV DNA. The transfections performed with the 3-kb RSV *src* DNA fragment in the absence of carrier DNA demonstrated that the transfecting DNA species could be inserted directly into the cell genome. We asked next whether transformation of NIH/3T3 mouse cells by transfection with cloned RSV DNA was absolutely dependent upon certain kinds of DNA sequences directly adjacent to viral DNA for expression of *src*, by transfecting cells with *Sac*I-permuted linear RSV DNA contained within the cloning vector λgtWES · λB DNA (Fig. 1E) in the absence of carrier DNA. Although the efficiency of transformation with intact recombinant DNA was considerably less than with *Sac*I-permuted RSV DNA freed of bacteriophage DNA (Table 1), analysis of DNA from a transformed line, λ-C, showed that the integrated RSV DNA remained flanked by extensive regions of λ phage DNA. At least 4.6 kb of vector DNA on the 5′ side of the RSV DNA and at least 7.5 kb on the 3′ side were intact (data not shown), with distal sites in the vector presumably linked directly to chromosomal DNA.

Synthesis of viral RNA in NIH/3T3 mouse cells transformed by transfection with various forms of cloned RSV DNA. In cells infected with retroviruses, the LTRs and other viral sequences regulate transcription of the provirus and processing of transcripts. Each of the transformed cell lines described above provides an opportunity to test current notions about the role of viral signals in the regulation of viral gene expression. The patterns of integration of cloned RSV DNA in the transformed cells described above indicate that the RSV LTR may be dispensable for controlling viral gene expression under certain circumstances. Cellular (host or carrier) DNA sequences adjacent to integrated viral DNA could function to control synthesis of viral RNA in these transformed cell lines.

Presented here are stable polyadenylated, virus-specific transcripts in three cell lines transformed with cloned RSV DNA: (i) the cell line S-d, which contains one integrated copy of the *Sac*I-permuted RSV genome, (ii) the cell line E-e, which harbors one integrated copy of the 3-kb subgenomic RSV DNA encoding *src*, and (iii) the cell line λ-C which has bacteriophage λ DNA flanking the *Sac*I-permuted form of RSV DNA.

Analysis of gel-fractionated RNA from cell line S-d with RSV *src* probe revealed two prominent closely spaced bands at 3.1 and 2.8 kb and a faint band at 9 kb (Fig. 7B). Only the 9-kb mRNA hybridized with probe specific for RSV *gag* sequences (Fig. 7C). Probe to RSV LTR-U3 sequences detected all three species (Fig. 7D); however, probe to the RSV LTR-U5 sequence hybridized to the 3.1-kb species and faintly to the 9-kb mRNA (not visible in the figure) but not to the 2.8-kb species (Fig. 7E). These findings are most readily interpreted by proposing that the 2.8-kb RNA is polyadenylated at the signal provided by the first LTR 3′ to *src* and that the 3.1-kb RNA is polyadenylated at the signal provided by the second LTR (Fig. 3). A candidate for RSV *env* mRNA was not detected in these experiments. Patterns of viral RNA in two additional transformed cell lines, each harboring one copy of the *Sac*I-permuted RSV genome, were very similar to that in cell line S-d (data now shown). The ratio of RSV *gag* mRNA to RSV *src* mRNA in these lines is similar to that in RSV-infected mammalian cells harboring a normal provirus (20).

RNA from cell line E-e, containing one integrated copy of the subgenomic RSV DNA fragment (Fig. 6), shows a 7-kb transcript that hybridizes with RSV-*src* probe (Fig. 7F). Below, we consider the contribution of host cell sequences to the termini of *src* mRNA in this cell line.

Cell line λ-C has the *Sac*I-permuted RSV DNA flanked with bacteriophage λ DNA. Hybridization of RNA from cell

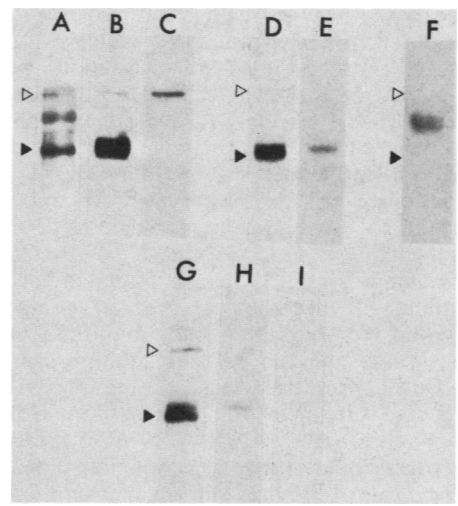

FIG. 7. Analysis of poly(A)-selected RNA in transfected cells. Poly(A)-containing RNA was prepared from chicken embryo fibroblasts infected with SR-A virus and from three transformed NIH/3T3 cell lines. RNA was electrophoresed on agarose-formaldehyde gels, transferred to nitrocellulose filters, and hybridized to RSV and bacteriophage probes. Lanes: A, RNA from SR-A-infected chicken embryo fibroblasts hybridized to RSV *src* probe; B through E, RNA from cell line S-d hybridized to RSV *src* probe (lane B), RSV *gag* probe (lane C), RSV-U3 probe (lane D), and RSV-U5 probe (lane E); F, RNA from cell line E-e hybridized to RSV *src* probe; G through I, RNA from cell line λ-C hybridized to RSV *src* probe (lane G), RSV-U5 probe (lane H), and bacteriophage λ probe (lane I). The solid triangle shows the position of the normal 2.8-kb v-*src* mRNA, and the open triangle indicates the position of 9-kb genomic viral RNA.

line λ-C with RSV-*src* probe shows a doublet at 3.1 and 2.8 kb and a faint band at 9 kb (Fig. 7G). The 9-kb transcript also hybridizes with RSV-*gag* probe (data not shown). RSV LTR-U5 probe hybridizes to the 3.1- and 9-kb transcripts (Fig. 7H; annealing to the 9-kb transcript is too faint to be seen in the figure). Notably, no hybridization was observed with bacteriophage λ DNA probe (Fig. 7I). The pattern of viral transcripts observed in cell line λ-C is thus similar to that in cell line S-d described above.

DISCUSSION

We have examined the assimilation and expression of various forms of cloned RSV DNA presented by transfection to nonpermissive NIH/3T3 mouse cells in culture. RSV LTR sequences were found not to direct integration of any of the forms of cloned RSV DNA. The integration patterns (Table 2) are in marked contrast to the structure of proviral DNA in cells infected with virus, and they inevitably affect the manner in which viral genes are expressed.

Effects of the form of RSV DNA upon RSV RNA. Linear RSV DNA, permuted with respect to the *Sac*I site and containing two LTR sequences, was found to integrate into cell DNA near its ends. In six transformed cell lines harboring only one RSV DNA insertion in cell DNA, the LTR sequences were downstream from the viral genes. Analyses of viral mRNA in these transformed cell lines are consistent with the notion that cellular sequences immediately upstream from the integrated RSV DNA provide both a signal for initiation of transcription and part of the leader sequence for *gag* and *src* mRNA molecules. Thus, the *src* message may have a composite host-viral leader sequence spliced to *src* sequences via the normal splice donor and acceptor sites (11, 26). It is also possible that initiation of transcription of viral genes in these cell lines occurs within the left-most RSV DNA sequences or just upstream of the *src* gene. Resolution of these issues will require a detailed analysis of the structure of the 5′ ends of these viral transcripts, as well as molecular cloning of host cell DNA adjacent to the 5′ end of the integrated RSV DNA. Poly(A) addition probably occurs at LTR sequences located downstream from the viral genes in cell lines transformed by *Sac*I-permuted DNA. Approximately one-fourth of the stable poly(A)-containing *src* mRNA appears to arise by reading through the first LTR into the adjacent LTR.

The subgenomic 3-kb RSV *Eco*RI fragment encoding the *src* gene contains the viral splice acceptor site upstream of *src* and the first 176 bp of the U3 region of the LTR but not the "TATA" box and the poly(A) addition signal of the LTR (25). Downstream from the *src* gene in this 3-kb DNA fragment is the "enhancer" element of RSV (15). Recent experiments indicate that the 3-kb RSV *Eco*RI fragment can induce sarcomas after direct injection into chicken wing webs (9); removal of the RSV enhancer from this fragment greatly reduces its ability to induce tumors in chickens (D. Robinson, P. A. Luciw, and H. J. Kung, unpublished data). Initiation of mRNA for $pp60^{src}$ in the cells transformed by the 3-kb *src* fragment probably occurs in cell DNA upstream of the integrated DNA. A mouse leader sequence could be joined to the normal splice acceptor site for *src* mRNA, located within the 3-kb *src* fragment, ca. 75 bp on the 5′ side of the *src* ATG (26). Mouse sequences probably also provide a signal and a site for poly(A) addition since the viral poly(A) addition sites are not located in the 3-kb *src* fragments. Analyses of *src* mRNA synthesis in these transformed cell lines revealed the presence of *src* transcripts much larger than 3 kb (e.g., Fig. 7F), suggesting that the messages are composites of RSV *src* sequences and NIH/3T3 mouse cell DNA sequences from both sides of the unintegrated viral DNA.

Transformed mammalian cells expressing $pp60^{src}$ were also obtained by transfecting NIH/3T3 mouse cells with the *Sac*I-permuted configuration of RSV DNA still contained within the cloning vector DNA λgtWES. Viral transcripts were readily detected in one such cell line (Fig. 7G to I); the transcripts resembled those seen in cells transformed by linear *Sac*I-permuted DNA and did not anneal to λ probes. The manner in which these species are generated is not known. It also remains to be determined whether the very low transformation efficiency of this chimeric DNA is due to the constraints imposed by the phage DNA on expression of the *src* gene or to an inhibitory effect of phage DNA similar to that described for biochemical transformation of tissue culture cells by transfection (28).

To improve the expression of viral genes by flanking them with LTR sequences as in natural infection, tandem arrays of the *Sac*I-permuted linear RSV DNA were prepared by ligation with T4 DNA ligase in vitro, and we observed a modestly increased efficiency of transformation (Table 1). Preliminary analyses of RSV RNA transcripts in a cell line transformed by transfection with tandem arrays revealed that the viral messages were similar in structure to the mRNA species in a cell line harboring a normal provirus (data not shown).

Formation and stability of tandem arrays. Ligation and recombination have been shown to occur between homologous and heterologous DNA molecules introduced into eucaryotic cells by various methods (8, 13, 18, 24). We observed tandem arrays containing only head-to-tail joinings in many transformed cell lines made by transfection with monomers of the *Sac*I-permuted RSV DNA and monomers of the 3-kb *Eco*RI DNA fragment encoding RSV *src*, with or without carrier DNA (Table 2). Large inverted repeats are unstable in bacteria due to the fact that replication cannot proceed normally. The analysis of integrated tandem arrays suggests that this may also be true in mammalian cells, especially since only the head-to-tail configuration was observed in cells transfected by a mixture of tandem arrays formed in vitro and shown to have a 2:1:1 molar ratio of head-to-tail, head-to-head, and tail-to-tail joinings before transfection. Selection against inverted repeats could account, at least in part, for the fact that only a moderate increase in transformation efficiency was observed when tandem arrays made in vitro were compared to monomers of the *Sac*I-permuted RSV DNA.

Integration of transfected DNA and relationship to the retrovirus life cycle. We have shown here that similar efficiencies of transformation are obtained with permuted linear and circular RSV DNA (Table 1) and that integration is not mediated through interactions with the LTRs. Thus, linear DNA is assimilated by recombination near the termini of permuted molecules (Fig. 3), and integrative recombination can occur at any of several sites in recircularized viral DNA, including sites external to the LTRs (Fig. 5). Similar results have been reported after microinjection of linear and circular retroviral DNA (8, 15), after transfection with DNA directly isolated from RSV-infected cells (4, 6), and after infection with a simian virus 40 vector containing the LTRs of a murine retrovirus (14). The failure of retroviral DNA introduced by these heterodox methods to integrate in response to sequences honored during natural infection implies that viral proteins accompanying parental genomes may have an essential role in the integrative mechanism.

ACKNOWLEDGMENTS

We wish to thank many colleagues, particularly Bill DeLorbe, Steve Hughes, John Majors, Art Levinson, Nancy Quintrell, Ron Swanstrom, and Suzanne Ortiz for advice, assistance, and materials. We are also grateful to Geoff Cooper for a supply of NIH/3T3 cells and to Janine Marinos for typing and in other ways facilitating the preparation of this manuscript.

Our work is supported by Public Health Service grants from the National Institutes of Health and by a grant from the American Cancer Society.

ADDENDUM IN PROOF

Panganiban and Temin (Cell **36**:673–679, 1984) have recently demonstrated that the probable precursor to the provirus during infection is circular DNA with two tandem LTRs.

LITERATURE CITED

1. **Anderson, P., M. P. Goldfarb, and R. A. Weinberg.** 1979. A defined subgenomic fragment of *in vitro* synthesized Moloney sarcoma virus DNA can induce cell transformation upon transfection. Cell **16**:63–75.
2. **Bishop, J. M.** 1978. Retroviruses. Annu. Rev. Biochem. **47**:35–88.
3. **Copeland, N. G., and G. M. Cooper.** 1979. Transfection by exogenous and endogenous murine retrovirus DNAs. Cell **16**:347–356.
4. **Copeland, N. G., N. A. Jenkins, and G. M. Cooper.** 1981. Integration of Rous sarcoma virus DNA during transfection. Cell **23**:51–60.
5. **Copeland, N. G., A. D. Zelenetz, and G. M. Cooper.** 1979. Transformation of NIH/3T3 mouse cells by DNA of Rous sarcoma virus. Cell **17**:993–1002.
6. **Copeland, N. G., A. D. Zelenetz, and G. M. Cooper.** 1980. Transformation by subgenomic fragments of Rous sarcoma virus DNA. Cell **19**:863–870.
7. **DeLorbe W. J., P. A. Luciw, H. M. Goodman, H. E. Varmus, and J. M. Bishop.** 1980. Molecular cloning and characterization of avian sarcoma virus circular DNA molecules. J. Virol. **36**:50–61.
8. **Folger, K. R., E. A. Wong, G. Wahl, and M. R. Capecchi.** 1982. Patterns of integration of DNA microinjected into cultured mammalian cells: evidence for homologous recombination between injected plasmid DNA molecules. Mol. Cell. Biol. **2**:1372–1387.
9. **Fung, Y.-K. T., L. B. Crittenden, A. M. Fadly, and H.-J. Kung.** 1983. Tumor induction by direct injection of cloned v-*src* DNA into chickens. Proc. Natl. Acad. Sci. U.S.A. **80**:353–357.
10. **Graham, F. L., and A. J. Van der Eb.** 1973. A new technique for the assay of infectivity of human adenovirus 5 DNA. Virology **52**:456–467.
11. **Hackett, P. B., R. Swanstrom, H. E. Varmus, and J. M. Bishop.** 1982. The leader sequence of the subgenomic mRNA's of Rous sarcoma virus is approximately 390 nucleotides. J. Virol. **41**:527–534.
12. **Hughes, S. H., P. R. Shank, D. H. Spector, H.-J. Kung, J. M. Bishop, H. E. Varmus, P. K. Vogt, and M. L. Brietman.** 1978. Proviruses of avian sarcoma virus are terminally redundant, coextensive with unintegrated linear DNA and integrated at many sites. Cell **15**:1397–1410.
13. **Kopchick, J. J., and D. W. Stacey.** 1984. Differences in intracellular DNA ligation after microinjection and transfection. Mol. Cell. Biol. **4**:240–246.
14. **Kriegler, M., and M. Botchan.** 1983. Enhanced transformation by a simian virus 40 recombinant virus containing a Harvey murine sarcoma virus long terminal repeat. Mol. Cell. Biol. **3**:325–339.
15. **Luciw, P. A., J. M. Bishop, H. E. Varmus, and M. R. Capecchi.** 1983. Location and function of retroviral and SV40 sequences that enhance biochemical transformation after microinjection of DNA. Cell **33**:705–716.
16. **Nusse, R., and H. E. Varmus.** 1982. Many tumors induced by the mouse mammary tumor virus contain a provirus integrated in the same region of the host genome. Cell **31**:99–109.
17. **Oppermann, H., A. D. Levinson, H. E. Varmus, L. Levintow, and J. M. Bishop.** 1979. Uninfected vertebrate cells contain a protein that is closely related to the product of the avian sarcoma virus transforming gene (*src*). Proc. Natl. Acad. Sci. U.S.A. **76**:1804–1808.
18. **Perucho, M., D. Hanahan, and M. Wigler.** 1980. Genetic and physical linkage of exogenous sequences in transformed cells. Cell **22**:309–317.
19. **Pulleybank, D. E., M. Shure, D. Tang, J. Vinograd, and H.-P. Vosberg.** 1975. Action of nicking-closing enzyme on supercoiled and nonsupercoiled closed circular DNA: formation of a Boltzmann distribution of topological isomers. Proc. Natl. Acad. Sci. U.S.A. **72**:4280–4284.
20. **Quintrell, N., S. H. Hughes, H. E. Varmus, and J. M. Bishop.** 1980. Structure of viral DNA and RNA in mammalian cells infected with avian sarcoma virus. J. Mol. Biol. **143**:363–393.
21. **Shank, P. R., S. H. Hughes, H.-J. Kung, J. E. Majors, N. Quintrell, R. V. Guntaka, J. M. Bishop, and H. E. Varmus.** 1978. Mapping unintegrated avian sarcoma virus DNA: termini of linear DNA bear 300 nucleotides present once or twice in two species of circular DNA. Cell **15**:1383–1395.
22. **Southern, E. M.** 1975. Detection of specific sequences among DNA fragments separated by gel electrophoresis. J. Mol. Biol. **98**:503–517.
23. **Stowe, N. D., and N. M. Wilkie.** 1976. An improved technique for obtaining enhanced infectivity with herpes simplex virus type 1 DNA. J. Gen. Virol. **33**:447–458.
24. **Subramani, S., and P. Berg.** 1983. Homologous and nonhomologous recombination in monkey cells. Mol. Cell. Biol. **3**:1040–1052.
25. **Swanstrom, R., W. DeLorbe, J. M. Bishop, and H. E. Varmus.** 1981. Nucleotide sequence of cloned unintegrated avian sarcoma virus DNA: viral DNA contains direct and inverted repeats similar to those in transposable elements. Proc. Natl. Acad. Sci. U.S.A. **78**:124–128.
26. **Swanstrom, R., R. C. Parker, H. E. Varmus, and J. M. Bishop.** 1983. Transduction of a cellular oncogene: the genesis of Rous sarcoma virus. Proc. Natl. Acad. Sci. U.S.A. **80**:2519–2523.
27. **Varmus, H. E., and R. Swanstrom.** 1982. "Replication of retroviruses," p. 369–512. *In* J. Coffin, N. Teich, H. E. Varmus, and R. Weiss (ed.), Molecular biology of tumor viruses, part III, RNA tumor viruses. Cold Spring Harbor Press, Cold Spring Harbor, N.Y.
28. **Yoder, J. I., and A. T. Ganesan.** 1983. Procaryotic genomic DNA inhibits mammalian cell transformation. Mol. Cell. Biol. **3**:956–959.
29. **Zasloff, M., G. D. Ginder, and G. Felsenfeld.** 1978. A new method for the purification and identification of covalently closed circular DNA molecules. Nucleic Acids Res. **5**:1139–1152.